Macromolecules

ARTICLE

pubs.acs.org/Macromolecules

Fabrication of Core−Shell Nanostructures from Near-Infrared Electrochromic Amphiphilic Diblock Copolymers Containing Pendant Dinuclear Ruthenium Group through Assembly and Their Optical, Electrochemical, and Electroptical Properties

Weiran Lin, Yijun Zheng, Jie Zhang,* and Xinhua Wan*

Beijing National Laboratory for Molecular Sciences, Key Laboratory of Polymer Chemistry & Physics of Ministry of Education, College of Chemistry & Molecular Engineering, Peking University, Beijing 100871, P. R. China

Supporting Information

ABSTRACT:

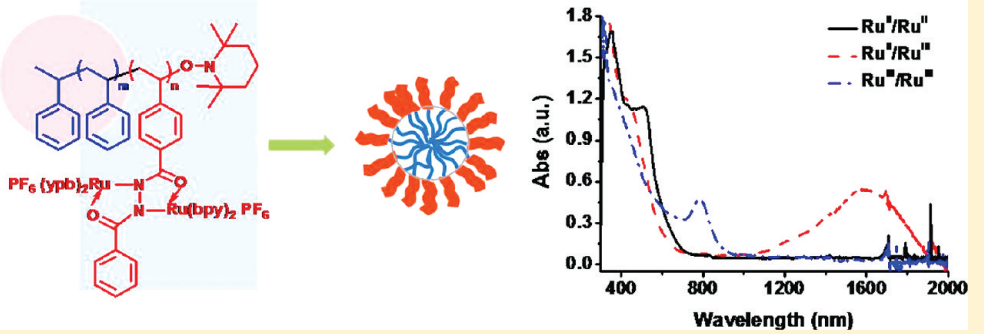

Novel well-defined diblock copolymers polystyrene-*b*-poly[benzoic acid *N*′-(4-vinylbenzoyl)hydrazide dinuclear ruthenium complex] (PS_m-*b*-P(DCH-Ru)$_n$, m = 2076, n = 417, 1024, 2432) are synthesized through two-step sequential nitroxide-mediated radical polymerization (NMRP) and postpolymerization complexation. The block copolymers containing pendant dinuclear ruthenium groups possess an amphiphilic nature. The assembly behavior of the complex block copolymers in both selective solvents acetonitrile and dioxane at various initial concentrations and block compositions were characterized by transimission electron microscopy (TEM). Spherical micelles and vesicles were observed in acetonitrile and dioxane, respectively. The photoluminescent, electrochemical, and spectroelectrochemical properties of the complex block copolymers in solution were investigated. The solvatochromism in the UV−vis region and electrochromism (EC) in the near-infrared region (NIR) were observed. Aggregates solutions in either acetonitrile or dioxane show quite different electroptical properties from that of the homogeneous solution in DMF, which might be due to spatial-confinement effect of the functional Ru pendent groups in core−shell nanostructures.

INTRODUCTION

Diverse nanostructures constructed through supramolecular self-assembly of electroactive and photoactive molecular building blocks can be endowed with electronic, optoelectronic, and photonic properties.[1−4] One approach to create building blocks is the incorporation of functional components into block copolymers. The amphiphilic block copolymers are capable to assemble into core−shell nanoscaled suprastructures in solution. It is known that the electro- or optical-active groups are sensitive to the microenvironment, and therefore the spatial-confinement effects within the core−shell nanostructures on their properties are crucial.[5,6] It opens up the opportunity for investigating the suprastructure−property relationship.

Organic near-infrared (NIR) optoelectronic materials are becoming more attractive due to their interesting electrical/optical properties and foreseeable applications in photonics, biological imaging, and telecommunications (e.g., for fiber-optic communications at the wavelengths of 1310 and 1550 nm).[7−10] The incorporation of NIR-active chromophores into block copolymer architectures capable of self-assembly can thus be expected to facilitate the creation of diverse, luminescent, and photonic nanostructures.[9] However, combining the fascinating self-assembly properties of block copolymers containing NIR-active components is still challenging due to absence of proper synthetic strategies, and up to date studies on their self-assembly and properties of their supramolecular assemblies are very rare.

Among several types of NIR-absorbing organic materials reported in the literature, such as stacked naphthalimide anion

Received: March 7, 2011
Revised: May 23, 2011
Published: June 08, 2011

radicals,[11] fused phorphyrin arrays,[12] doped polythiophenes, and other related conducting polymers,[13] sandwich-type lanthanide bis(phthalocyanine)s,[14,15] and radical anions of conjugated diquinones (also called semiquinones),[16] a family of mixed-valence dinuclear ruthenium complexes with various bridging ligands is particularly interesting as a new class of NIR organic materials.[17−25] The early work by Kaim, Wang, and their co-workers has revealed that the ruthenium complexes with 2,2′-bipyridine (bpy) and dicarbonylhydrazine (DCH) ligands are electrochromic (EC) in the NIR region.[18−20] DCH−Ru complexes can exist in three forms depending on the oxidation state of ruthenium metals: Ru^{II}/Ru^{II}, Ru^{II}/Ru^{III}, and Ru^{III}/Ru^{III}. Accordingly, the absorption bands are typically centered at 550 nm (Ru^{II}/Ru^{II}), 800 nm (Ru^{III}/Ru^{III}), and 1600 nm (Ru^{II}/Ru^{III}) and assigned to the metal-to-ligand charge transfer (MLCT), ligand-to-metal charge transfer (LMCT), and metal-to-metal charge transfer (MMCT) transitions. Such a series of complexes are stable toward strong base (e.g., NaOH), water, air, and high temperature. Qi et al. had successfully introduced the DCH−Ru moieties into the polymer main chain through post-polymerization complexation method.[26] We also reported the conventional radical copolymerization of a series of polymers containing DCH ligands as pendent groups and also investigated the interesting NIR EC, photoluminescent (PL), and electroluminescent (EL) properties of the complex polymers containing dinuclear ruthenium synthesized through the postpolymerization route.[27]

Herein, we report the incorporation of the NIR active DCH−Ru group into block copolymers via combining sequential nitroxide-mediated radical polymerization and postpolymerization complexation. The self-assembly behaviors of the amphiphilic complex block copolymers in acetonitrile and dioxane with different initial concentrations and block compositions were studied, and the spatial-confinement effects in those core−shell nanostructures on the solvatochromic, photoluminescent, electrochemical, and electroptical properties of block copolymers were investigated.

EXPERIMENTAL SECTION

Materials. The monomer benzoic acid *N*′-(4-vinylbenzoyl)hydrazide (DCH), the initiator 1-phenyl-1-(2′,2′,6′,6′-tetramethyl-1′-piperidinyloxy)-ethane (PTEMPOE), and the complex reagent *cis*-$Ru(bpy)_2 \cdot 2H_2O$ were synthesized according to refs 27−29, respectively. Styrene (Beijing Chemical Reagents Co., 99.5%) was purified to remove the inhibitor by passing through a column of basic alumina, distilled out under vacuum, and kept in refrigerator. Chlorobenzene (Beijing Chemical Reagents Co., 99.5%) was refluxed over CaH_2 under argon overnight and then distilled out before use. Dimethylformamide (DMF, Beijing Chemical Reagents Co., 99.5%) was purified by refluxing with Linde type 4A molecular sieves under argon, followed by distillation under reduced pressure. Tetrahydrofuran (THF, 99.5%), cyclohexane (99.5%), methanol (99.5%), ether (99.5%), and acetone (99.5%) were all purchased from Beijing Chemical Reagents Co. and used as received. Acetonitrile (Tianjin Shield Co., HPLC grade) and tetra-*n*-butylammonium hexafluorophosphate (Bu_4NPF_6) (Acros) were used as received. All manipulations involving air-sensitive reagents were performed under an inert atmosphere.

Measurements. ^1H NMR (400 MHz) spectra were recorded on a Bruker ARX 400 spectrometer using deuterated chloroform ($CDCl_3$) as the solvent for the PS macroinitiators and the mixture of $CDCl_3$ and deuterated dimethyl sulfoxide (DMSO-d_6) for the ligand block copolymers with tetramethylsilane as the internal standard. The number-average molecular weights (M_n), weight-average molecular weights (M_w), and polydispersity indices (PDI = M_w/M_n) of all polymers were estimated by a gel permeation chromatography (GPC) apparatus equipped with a Waters 2410 refractive-index detector and a Waters 515 pump at 35 °C, using monodispersed polystyrene as standards and DMF/0.1 M LiCl as the eluent at a flow rate of 1.0 mL/min. The compositions of ligand block copolymers were also measured by elemental analyses, performed on an Elementar Vario EL instrument.

Profile Spec inductively coupled plasma atomic emission spectroscopy (ICP-AES, Leeman Laboratories) was employed to determine the ruthenium contents in the Ru-containing block copolymers. The complex block copolymer samples were refluxed with concentrated nitric acid (65−68%) for about 2 h and diluted to 2 wt % HNO_3 content with the ruthenium content more than 10 μg/mL right before the measurement.

The PL spectra were collected on Hitachi F4500 fluorescence spectrum analyzer. The electrochemical measurements were carried out on a CHI 840B electrochemical workstation with glassy carbon electrodes against a silver pseudoreference electrode. The cyclic voltammograms (CV) of PS_{2076}-*b*-P(DCH-Ru)$_n$ block copolymers in solutions were directly collected in the nitrogen-saturated solution of 0.1 mol/L hexafluorophosphate (Bu_4NPF_6, TBAH), while that of the block copolymer films prepared by casting polymer solution onto a glassy carbon electrode were monitored in D_2O with 0.1 mol/L LiCl. All the electrochemical measurements were referenced to Ag/Ag^+. The pseudoreference was calibrated externally using a 5 mM solution of ferrocene (Fc/Fc^+). The UV−vis−NIR absorbance spectra were collected on a Shimadzu UV 3100 UV−vis−NIR spectrophotometer. The spectroelectrochemical experiments were performed in an optical transparent thin layer (OTTLE) cell with platinum electrode against a silver pseudoreference electrode. The spectroelectrochemical spectra of Ru-containing block copolymers in solution were measured with 0.1 mol/L TBAH in dry DMF or acetonitrile as electrolytic solution, while that of the block copolymer films prepared by casting polymer solution onto an ITO anode were measured with 0.1 mol/L LiCl in D_2O as electrolytic solution. Transmission electron microscopy (TEM) images were recorded on a JEM-200CX TEM operating at an acceleration voltage of 120 kV.

Synthesis of a Polystyrene Macroinitiator (PS-TEMPO). An appropriate amount of the PTEMPOE initiator, styrene, and chlorobenzene were mixed in a dry glass tube. After three freeze−pump−thaw cycles, the tube was sealed under vacuum and put into an oil bath thermostated at 125 ± 0.5 °C. The polymerization was terminated before the monomer conversion reached 50%. The reactant solution was diluted with THF and then added slowly into a large amount of methanol to precipitate the polymer. To remove the unreacted monomers completely, dissolution in THF and precipitation in methanol was repeated for three times. Finally, the white products were dried under vacuum at room temperature.

Sequential Polymerization for Ligand Diblock Copolymers Polystyrene-*block*-Poly[benzoic acid *N*′-(4-vinylbenzoyl)-hydrazide]. The polymerization procedure of ligand block copolymers was similar to that of PS-TEMPO described above, with PS-TEMPO as the macroinitiator, benzoic acid *N*′-(4-vinylbenzoyl)hydrazide (DCH) as the monomer, and DMF as the solvent. At the end of the polymerization, the unreacted PS macroinitiator was removed by a continuous extraction process for 5 days with cyclohexane as an extraction solvent using a Soxhlet extraction apparatus. Finally, the white products were thoroughly dried under vacuum at room temperature. The homopolymer P(DCH) was obtained with the same procedure as above except for the PTEMPOE initiator instead of PS-TEMPO.

A General Procedure for Complexation of the Ligand Block Copolymer with Ruthenium.[12,17]. A solution of *cis*-$Ru(bpy)_2Cl_2 \cdot 2H_2O$ (0.067 g, 0.13 mmol), ligand block copolymer (0.064 mmol per DCH group, according to the elemental analysis), and sodium carbonate (0.019 g, 0.018 mmol) in DMF (15 mL) was heated to reflux for 48 h under

dx.doi.org/10.1021/ma200516q |*Macromolecules* 2011, 44, 5146–5154

Scheme 1. Schematic Representatives of Synthetic Route of Block Copolymers PS_m-*b*-$P(DCH)_{n-x}$-$P(DCH\text{-}Ru)_x$ and the Chromophore Arrangement on the Backbone of the P(DCH-Ru) Block

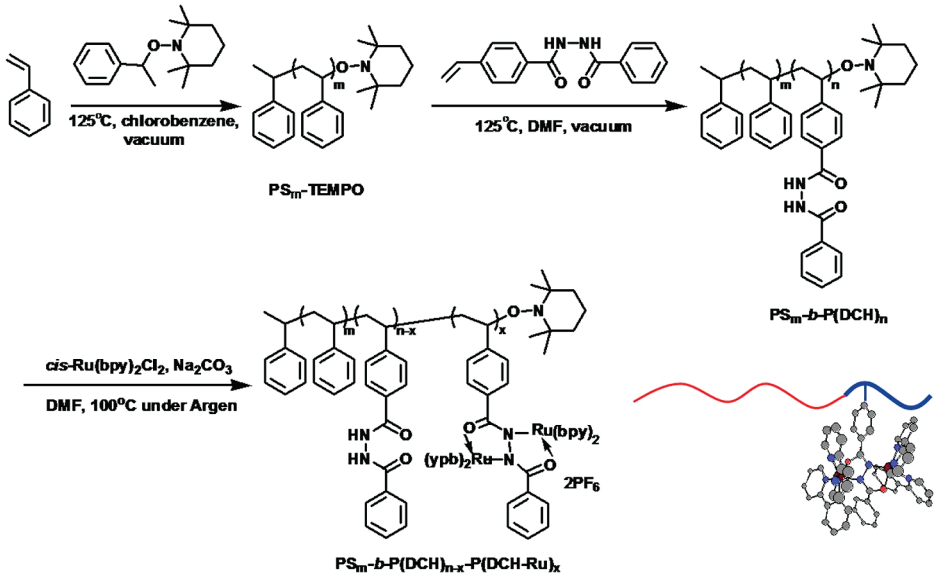

argon. After cooling to room temperature, a solution of ammonium hexafluorophosphate (1.0 g in 35 mL of water) was added. The red dark precipitate was filtered off and redissolved in acetone (20 mL). The ruthenium complex was then precipitated out with ether and dried under vacuum at room temperature (60% yield).

Preparation of Complex Block Copolymer Aggregates. The diblock copolymer PS_m-*b*-$P(DCH\text{-}Ru)_n$ were first dissolved in DMF to give a homogeneous solutions with various concentrations (0.1−2.0 wt %). Then the selective solvent acetonitrile or dioxane was added at a constant rate (0.25 wt % /min) under vigorous stirring until 40 wt % of a selective solvent content was reached. The resulting micellar solution was stirred for about 5 h and then dialyzed (the cutoff M_w ~4 kDa) against the selective solvent to remove DMF. The dialysate was changed every 6 h over a period of 3 days. For TEM experiments, a drop of the aggregate solution after dialysis was deposited onto a carbon-coated copper grid for a few minutes. Excess solution was blotted away with a strip of filter paper, and the sample grid was dried in air at room temperature. The dinuclear Ru-containing blocks could provide sufficient contrast for TEM observation without negative staining.

RESULTS AND DISCUSSION

Synthesis and Characterization of Ru-Containing Block Copolymers. There are generally two routes to produce the ruthenium complex polymers. One is to directly polymerize a Ru complex monomer. Another route is based on postpolymerization or polymer transformation and involves the synthesis of the ligand polymer and subsequent complexation with $Ru(bpy)_2Cl_2$. The polymerization reactivity of the ruthenium complex monomer, (benzoic acid *N*′-(4-vinylbenzoyl)hydrazide)$[Ru(bpy)_2]_2$, was tested under a typical NMRP initiating system, and only oligomers with a low yield were obtained. Consequently, we chose the postpolymerizaiton route in the present work (Scheme 1).

A series of well-defined ligand diblock copolymers PS_m-*b*-$P(DCH)_n$ (*m* and *n* denote the degree of polymerization of PS and DCH, respectively) were prepared by NMRP reactions with the sequential addition of monomers. After the first step of sequential living polymerizations, the PS-TEMPO macroinitiator can be obtained with a low polydispersity index of 1.15 and average M_n of 160 kDa. The ligand monomer DCH has a comparable structure to the styrene analogues and has been testified to possess good reactivity through the NMRP controlled polymerization (Supporting Information Figure S1). Therefore, the ligand blocks with different lengths were synthesized upon varying the feed ratio of the monomer to the PS-TEMPO macroinitiator. As a result, the diblock copolymers PS_m-*b*-$P(DCH)_n$ have monodispersities of 1.2−1.4 indicated by GPC in DMF/0.1 M LiCl as an eluent (see Figure S2). The element analysis indicates the exact copolymer compositions of ligand block copolymers PS_m-*b*-$P(DCH)_n$ (m = 2076; n = 417, 1024, and 2432). ^{1}H NMR measurements further confirm the chemical structures of all the copolymers (see Figure S3).

The complex block copolymers were synthesized through the ligand-exchange method with *cis*-$Ru(bpy)_2Cl_2 \cdot 2H_2O$ according to the procedure described in previous work.[17,22] Since the ligand polymers are stable against degradation under the same complexation conditions, the number-average repeating units of the P(DCH-Ru) blocks are considered to be equal to those of the ligand block copolymers. The ruthenium contents in complex block copolymers were determined by ICP analysis. As summarized in Table 1, the complex ratio was calculated by comparing the practical weight content of Ru atom in the complex block copolymer to the theoretical value for complete complexation. The practical Ru contents of the complex block copolymers did not reach the theoretical values probably due to the conformation change of the ligand block through the complexation. The rigidity of the ligand block might increase remarkably after the complexation of the pendant Ru complex groups due to the stronger steric hindrance and electrostatic repulsion between neighboring bulky Ru complex side groups. For simplicity, PS_m-*b*-$P(DCH\text{-}Ru)_n$ is used to denote the fine chemical structure of PS_m-*b*-$P(DCH)_{n-x}$-$P(DCH\text{-}Ru)_x$.

Assembly Behavior of Complex Block Copolymers. The block copolymers PS_m-*b*-$P(DCH\text{-}Ru)_n$ possess an amphiphilic

dx.doi.org/10.1021/ma200516q |*Macromolecules* 2011, 44, 5146–5154

Table 1. Summary of Characteristic Data of the Homopolymer $P(DCH)_{319}$ and the Ligand Block Copolymers PS_m-*b*-$P(DCH)_n$ and PS_m-*b*-$P(DCH\text{-}Ru)_n$

samples[a]	$M_{n,EA}$[c] ($\times 10^4$)	PDI[d]	DCH (wt %)	complex copolymers	Ru contents (%)[e]	complex ratio (%)[f]
$P(DCH)_{319}$[b]		1.22	100	$P(DCH\text{-}Ru)_{319}$	12.6	68.3
PS_{2076}-*b*-$P(DCH)_{417}$	32.68	1.38	33.9	PS_{2076}-*b*-$P(DCH\text{-}Ru)_{417}$	7.8	57.0
PS_{2076}-*b*-$P(DCH)_{1024}$	48.83	1.38	55.8	PS_{2076}-*b*-$P(DCH\text{-}Ru)_{1024}$	11.1	79.4
PS_{2076}-*b*-$P(DCH)_{2432}$	86.28	1.26	75.0	PS_{2076}-*b*-$P(DCH\text{-}Ru)_{2432}$	11.6	67.3

[a] The subscripts indicate the degrees of polymerization. The block ratio of the block copolymer was calculated by the element analysis. [b] The subscript of the homopolymer indicates the degree of polymerization determined by GPC with DMF/0.1 M LiCl as an eluent (RI detector, calibrated with polystyrene standards). [c] Number-average molecular weight obtained from element analysis. [d] The PDIs polydispersity distribution index (M_w/M_n) were determined by GPC with DMF/0.1 M LiCl as the eluent with monodispersed polystyrenes as standards. [e] Ru contents were determined by ICP analysis. [f] The complex ratio equals to the ratio of the practical weight content of Ru atom in the complex block copolymer characterized by ICP to the theoretical value.

Table 2. Summary of Characteristic Data of the Morphologies and Sizes of Nanoparticles from Block Copolymers PS_m-*b*-$P(DCH\text{-}Ru)_n$ at Various Conditions

		morphology and size of nanoparticles[b]	
samples	initial concn (wt %)	in acetonitrile	in dioxane
PS_{2076}-*b*-$P(DCH)_{417}$	0.01	–	S, 38 nm
PS_{2076}-*b*-$P(DCH)_{417}$	0.1	S,[a] 25 nm	V,[a] 120 nm
PS_{2076}-*b*-$P(DCH)_{417}$	0.5	S, 31 nm	–
PS_{2076}-*b*-$P(DCH)_{417}$	1.0	S, 35 nm	V, 100 nm
PS_{2076}-*b*-$P(DCH)_{417}$	2.0	S, 60 nm	V, 320 nm
PS_{2076}-*b*-$P(DCH)_{1024}$	1.0	S, 40 nm	V, 140 nm
PS_{2076}-*b*-$P(DCH)_{2432}$	1.0	S, 50 nm	V, 150 nm

[a] S stands for spherical micelles and V for vesicles. [b] The sizes of nanoparticles means the average diameters obtained from TEM images.

nature with the great disparity in both polarity and solubility between PS and Ru-containing blocks. To fabricate the dinuclear Ru^{II} complex chromophores into nanoscaled structures and understand the relationship between electroptical properties and aggregates structures, the assembly behavior of the complex block copolymer was investigated in DMF, acetonitrile, and dioxane with various solvent natures. DMF is the cosolvent for both blocks, while dioxane is the selective solvent for the PS block and acetonitrile is the selective solvent for the Ru-containing block.[26] Formation of aggregates of the complex block copolymers was induced by adding either acetonitrile or dioxane into DMF solution. The remnant common solvent DMF was further removed by dialysis against the corresponding selective solvent. The morphologies and sizes of nanoparticles were investigated by TEM, and all results are summarized in Table 2.

As shown in Figure 1, spherical micelles of block copolymer PS_{2076}-*b*-$P(DCH\text{-}Ru)_{417}$ with average diameters ~35 nm in acetonitrile solution were observed at 1.0 wt % initial concentration. Block copolymer compositions have little effects on the morphologies formed by complex block copolymers in acetonitrile. The average diameter of the micelles obviously increase with the length of Ru-containing block from 35 nm for PS_{2076}-*b*-$P(DCH\text{-}Ru)_{417}$ to 50 nm for PS_{2076}-*b*-$P(DCH\text{-}Ru)_{2432}$. The dependence of aggregate structures on the initial concentration of PS_{2076}-*b*-$P(DCH\text{-}Ru)_{417}$ was also studied. As shown in Figure 2, at the 0.1 wt % initial concentration of the copolymer in acetonitrile, uniform spherical micelles with an average diameter of 25 nm were formed. As the initial concentration increases to 0.5 wt %, micelles grow up to about 31 nm. Further increasing the initial concentration results in an increase of the micelle size. As the concentration is as high as 2.0 wt %, the large micelles with an average diameter of ~60 nm took the overwhelming majority under TEM observation. On the other hand, vesicles of complex block copolymers with diameters 80–200 nm with a broad size polydispersity were observed in dioxane, as depicted in Figure 1. Block copolymer compositions show no obvious effects on the size and morphology of aggregates. The dependence of aggregate morphologies of PS_{2076}-*b*-$P(DCH\text{-}Ru)_{417}$ in dioxane on initial concentrations were studied by TEM, as shown in Figure 1D–F. Uniform spherical micelles with an average diameter of ~38 nm were observed at an initial concentration of 0.01 wt %. Increasing the initial concentration to 0.1 wt % resulted in the formation of vesicles. As the initial concentration further increases to 2.0 wt %, porous spheres with an average diameter of ~100 nm appears, which are different from above aggregates . The aggregates formed in acetonitrile are quite different in structures from that in dioxane. In the simplified core–shell model, when dioxane is used as the selective solvent, the insoluble Ru-containing blocks would take constrained conformations in the core to minimize the free energy, while the soluble PS blocks extend outside in the corona to stabilize the whole aggregates. While in the case of acetonitrile as the selective solvent, the soluble Ru-containing blocks stay outside in the corona of spherical micelles. Owing to the steric hindrance and the repulsive interaction between the charged side groups, the rigidity of the Ru-containing block should be higher than that in dioxane.[30,31]

UV–vis Absorption and Solvatochromism of the Copolymer Solutions. The homogeneous solutions of PS_{2076}-*b*-$P(DCH\text{-}Ru)_n$ in DMF is red (inset of Figure 3A). The maximal absorptions of all complex block copolymers in the UV–vis region were peaked at around 500 nm, which are quite similar to the homopolymer (Figure 3). This absorption band is assigned to the $d\pi$ (Ru)–π^* (bpy) MLCT transition.[18,23] The maximal absorption was slightly blue-shifted as the Ru-containing block length increases (Table 3).

As the aggregates formed in either acetonitrile or dioxane, the polymer solution displays obvious solvatochromism. The solution color changes to orange in acetonitrile (inset of Figure 3B) or deep green in dioxane (inset of Figure 3C), different from that in DMF (inset of Figure 3A). The UV–vis absorbance spectra of the aggregate solution validate the color changes. Compared with the results from DMF solution, the maximal absorption of block

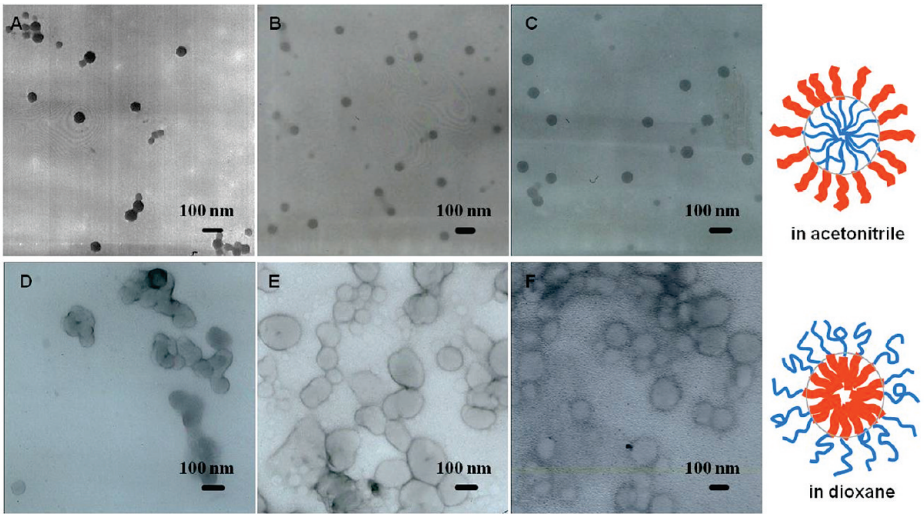

Figure 1. Morphologies obtained from the complex block copolymers with different compositions in acetontitrile: (A) PS_{2076}-*b*-$P(DCH\text{-}Ru)_{417}$, (B) PS_{2076}-*b*-$P(DCH\text{-}Ru)_{1024}$, and (C) PS_{2076}-*b*-$P(DCH\text{-}Ru)_{2432}$. Primary micelles obtained from complex diblock copolymers with different compositions in dioxane: (D) PS_{2076}-*b*-$P(DCH\text{-}Ru)_{417}$, (E) PS_{2076}-*b*-$P(DCH\text{-}Ru)_{1024}$, and (F) PS_{2076}-*b*-$P(DCH\text{-}Ru)_{2432}$. The initial concentration is 1.0 wt % in all cases. Schematical core−shell structure of the aggregates formed in dioxane and acetonitrile. The red line represents the Ru containing block, while the blue line represents the PS block.

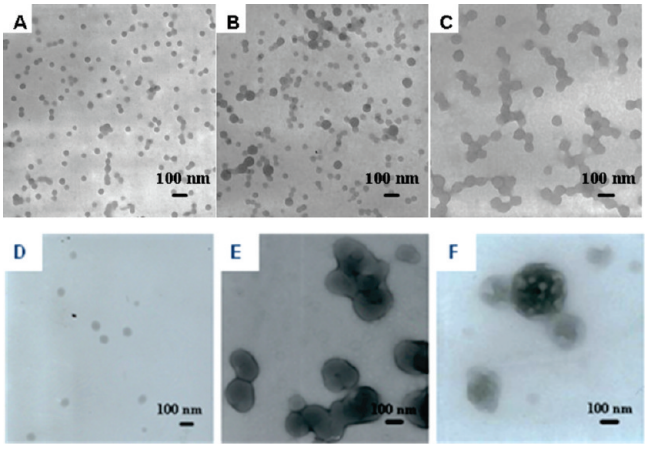

Figure 2. Primary micelles obtained from the complex diblock copolymer PS_{2076}-*b*-$P(DCH\text{-}Ru)_{417}$ through adding acetonitrile dropwisely into copolymer/DMF solutions at the initial concentration of 0.1 (A), 0.5 (B), and 2.0 wt % (C). Aggregate morphologies obtained from the complex diblock copolymer PS_{2076}-*b*-$P(DCH\text{-}Ru)_{417}$ through adding dioxane dropwisely into copolymer/DMF solutions at the initial concentration of 0.01 (D), 0.1 (E), and 2.0 wt % (F).

copolymers in acetonitrile shows a slight blue shift at the same DCH-Ru group concentration to 493 nm. In contrast, the absorption is significantly red-shifted to 700 nm in dioxane. In dioxane, the insoluble Ru-containing blocks with condensed conformations stay packed closely in the aggregate core. The strong intermolecular interaction between Ru-$(bpy)_2$ pendant groups might induce J-aggregation of bpy ligands of the Ru-containing block,[32] i.e., $\pi-\pi$ stacking between bpy ligands leads to orbit splitting of its exciton into the higher level and the lower one; the transition to the higher one was forbidden. Therefore, the MLCT transition energy decreases, which results in a red shift of the corresponding absorption. With regarding to the block copolymers in acetonitrile, the solvated P(DCH-Ru) blocks extended outside the shell layer and intermolecular interactions between neighborhood blocks could be negligible; therefore, their characteristic absorption is quite similar to that of the homopolymer. Such a result interprets that in a spatial-confined microenvironment the Ru-containing block has a great effect on the MLCT.

Photoluminescence. The aggregate solution of complex block copolymers exhibited obvious luminescence at room temperature in acetonitrile (5.0×10^{-4} mg/L) under excitation light of 520 nm as well as the homopolymer. The PL spectra for the complex block copolymers are virtually identical with an emission peaked at around 790 nm (Figure 4), which was consistent with the values previously reported for DCH-Ru complexes and random copolymers in acetonitrile.[18−21,27] The excited-state metal-to-ligand (MLCT) transition of ruthenium-containing copolymers should be responsible for the observed NIR PL.[33] While in the case of polymer solution in dioxane, luminescence was very weak with a low signal-to-noise ratio. As the Ru-containing blocks pack closely in the interior core of vesicular shells in dioxane, the local chromophore concentrations are too high, which induce self-quenching of the fluorescence. In contrast, all homopolymers and complex block copolymers exhibited no fluorescence at room temperature in DMF homogeneous solution, which might ascribe to fluorescence quenching due to the relatively high polarity of DMF and its better solubility to the Ru-containing block.

Electrochemical and Electrochromic Studies in Polymer Solutions. Cyclic voltammetric (CV) measurements of the complex copolymer and solutions were carried out by using Pt/C electrodes against a silver pseudoreference electrode with nitrogen-purged 0.1 M Bu_4NPF_6 solution as a supporting electrolyte. Figure 5A1 shows the cyclic voltammograms of the complex block copolymer PS_{2076}-*b*-$P(DCH\text{-}Ru)_{417}$ in DMF. The two redox couples are observed in the positive potential region corresponding to the two-step oxidation process: Ru^{II}-DCH-Ru^{II} ↔ Ru^{II}-DCH-Ru^{III} ↔ Ru^{III}-DCH-Ru^{III}. The electrochemical measurement results are summarized in Table 3.

dx.doi.org/10.1021/ma200516q |*Macromolecules* 2011, 44, 5146–5154

The gap between the two oxidation potentials (ΔE) is about 0.55 V, which is similar to those of other dinuclear DCH-Ru complexes[21,27] and the homopolymer (Figure 5C).

In reference to the redox potentials ($^1E_{1/2}$ and $^2E_{1/2}$) of PS_{2076}-*b*-$P(DCH\text{-}Ru)_{417}$, the spectroelectrochemical properties of the complex polymers in DMF were studied by using an OTTLE cell with different potentials. The absorption spectra in three redox states are shown in Figure 5A2. PS_{2076}-*b*-$P(DCH\text{-}Ru)_{417}$ in the Ru^{II}/Ru^{II} state displays two intense absorptions at around 350 and 505 nm, which are associated with the MLCT transition. Oxidation to the Ru^{II}/Ru^{III} state results in the appearance of a strong and broad intervalence transition band centered at 1600 nm. These bands are attributed to the MMCT transition formed in the mixed-valence state. Upon further oxidation to the Ru^{III}/Ru^{III} state, a new band at 800 nm appears which is assigned to the LMCT transition. These results indicate that the complex copolymers are NIR electrochromic.

With regard to the aggregate solution of PS_{2076}-*b*-$P(DCH\text{-}Ru)_{417}$ in acetonitrile, the CV results and the absorption spectra of the Ru^{II}/Ru^{III} and Ru^{III}/Ru^{III} states were similar to that of the copolymer in DMF homogeneous solutions and the homopolymer, indicating that aggregation had little effect on the MMCT and LMCT transition. It should be mentioned that the external voltage would cause the slow precipitation of the aggregates in acetonitrile, which may be owing to less solubility of Ru^{III} than Ru^{II} complexes. However, the electrochemical measurements could not be performed with the aggregate solution in dioxane because of the insolubility of electrolytes.

Electrochemical and Electrochromic Studies of Polymer Films. The above results illustrate that it is not applicable to investigate the electrochromic properties in solutions due to the limited solubility of aggregates of the block copolymers. Therefore, the same electrochemical measurements were carried out with thin films of the aggregates of block copolymer PS_m-*b*-$P(DCH\text{-}Ru)_n$ in acetonitrile and dioxane. The films were prepared by casting the aggregate solution onto a glassy carbon electrode for CV or an ITO anode for spectroelectrochemical measurement and drying under air. The 0.1 M TBAH/D_2O was employed as the electrolyte solution. The CV and absorption spectra of the aggregate film from acetonitrile as shown in Figure 6 were similar to that in solution. But the films made

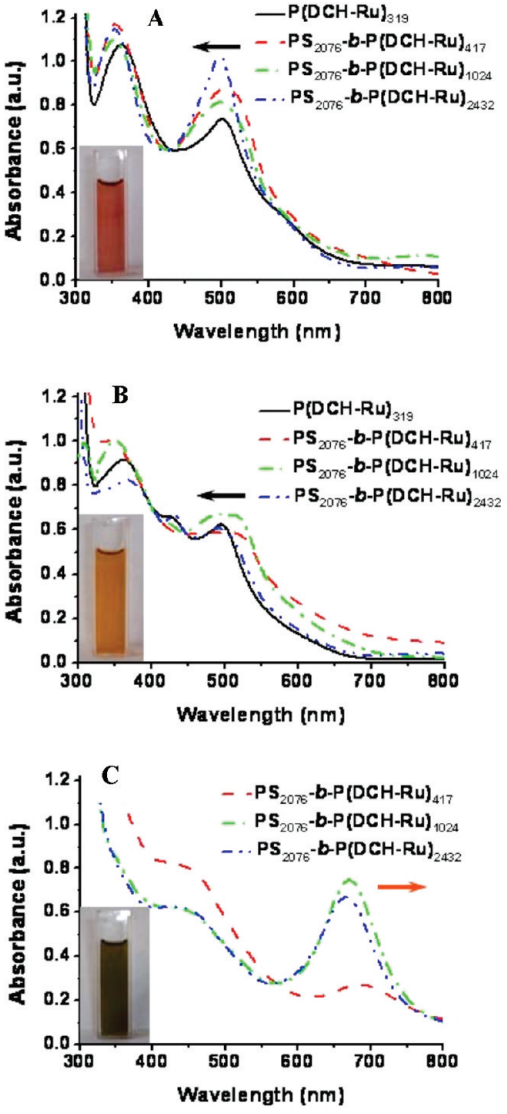

Figure 3. UV−vis absorbance spectra of the complex homopolymer and block copolymers PS_{2076}-*b*-$P(DCH\text{-}Ru)_n$ in (A) DMF, (B) acetonitrile, and (C) dioxane with a concentration of 0.01 wt %; insets in three figures are images of polymer solutions of PS_{2076}-*b*-$P(DCH\text{-}Ru)_{417}$ in the above three different solvents.

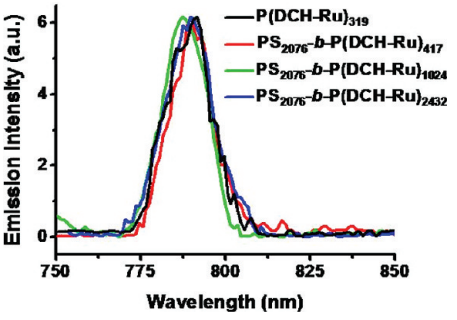

Figure 4. Emission spectra of complex homopolymer and block copolymer PS_{2076}-*b*-$P(DCH\text{-}Ru)_n$ in acetonitrile at an excitation wavelength of 520 nm.

Table 3. Characteristic Results of Complex Ratio and Optical Properties of Complex Block Copolymers PS_{2076}-*b*-$P(DCH\text{-}Ru)_n$

samples	$\lambda_{max,DMF}$[a] (nm)	$^1E_{1/2,DMF}$[b] (V)	$^2E_{1/2,DMF}$[b] (V)	$\lambda_{max,Ace}$ (nm)	$^1E_{1/2,Ace}$ (V)	$^2E_{1/2,Ace}$ (V)	$\lambda_{max,Dio}$ (nm)
$P(DCH\text{-}Ru)_{319}$-TEMP	502	0.53	1.09	495	0.52	1.08	
PS_{2076}-*b*-$P(DCH\text{-}Ru)_{417}$	505	0.54	1.10	501	0.53	1.08	700
PS_{2076}-*b*-$P(DCH\text{-}Ru)_{1024}$	500	0.53	1.09	493	0.53	1.06	660
PS_{2076}-*b*-$P(DCH\text{-}Ru)_{2432}$	499	0.53	1.08	493	0.53	1.08	663

[a] λ_{max} denotes the maximum absorption in visible region. [b] Cyclic voltammetry performed at a 100 mV/s scan rate in DMF/0.1 M TBAH. Potentials *E* in V vs NHE.

dx.doi.org/10.1021/ma200516q |*Macromolecules* 2011, 44, 5146–5154

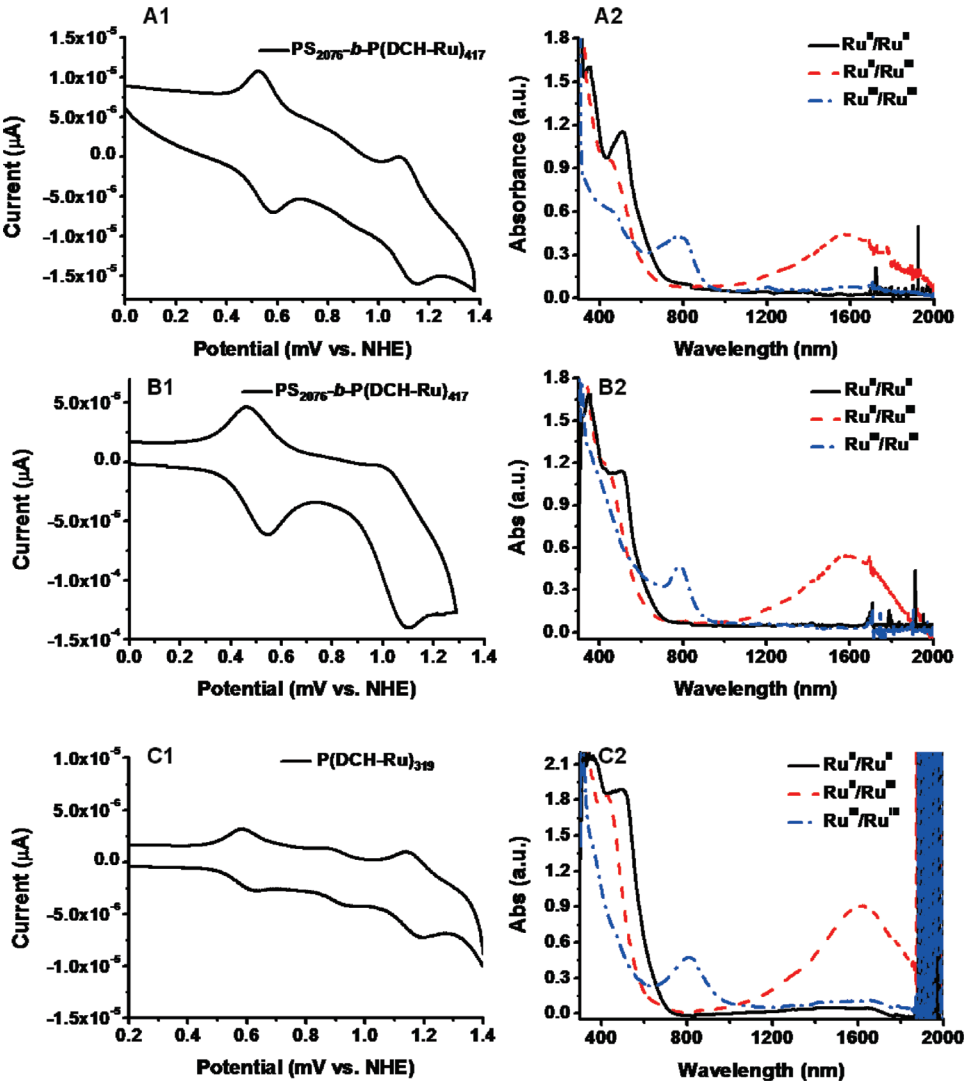

Figure 5. (A1) Cyclic voltammogram in DMF at a scan rate of 100 mV/s (with 0.1 M TBAH) and (A2) absorption spectra of complex block copolymer PS_{2076}-*b*-$P(DCH\text{-}Ru)_{417}$ in three oxidation states obtained in DMF using the OTTLE cell (with 0.1 M TBAH). Cyclic voltammogram (B1) and absorption spectra (B2) of complex block copolymer PS_{2076}-*b*-$P(DCH\text{-}Ru)_{417}$ in acetonitrile, were obtained at the same condition as above in DMF. Cyclic voltammogram (C1) and absorption spectra (C2) of the homopolymer $P(DCH\text{-}Ru)_{319}$ in acetonitrile were obtained at the same condition as above.

from the aggregate solution in dioxane showed no response to the external voltage because the insulation of PS blocks packed in the corona of the aggregates prevents the charge transfer from the electrolyte solution to the Ru-containing blocks.

The optical attenuation was recorded at one of the NIR wavelength of 1600 nm with stepping potentials between −0.3 and +0.8 V (Figure 7). The homopolymer films cast from the DMF and acetonitrile solution display a relatively low attenuation to 0.5 dB. The PS_{2076}-*b*-$P(DCH\text{-}Ru)_{417}$ film cast from the solution in DMF reaches 0.8 dB with a long switching time of about 30 s due to the nonconjugated nature of the copolymer backbone. In comparison to above films made from homogeneous solutions containing nonassembled P(DCH-Ru), the PS_{2076}-*b*-$P(DCH\text{-}Ru)_{417}$ film cast from the aggregate solution in acetonitrile obviously achieves better attenuation to 2.1 dB.

Such a better performance of PS_{2076}-*b*-$P(DCH\text{-}Ru)_{417}$ film from the acetonitrile solution might be attributed to its core—shell nanostructure: as we mentioned above, PS segments will block the charge transport in the redox processes. In the case of the nanostructure in dioxane with PS blocks extended in the shell, the outside PS block will prevent the charge transport to the interior Ru core, and therefore the nanostructure film displays no optical attenuation. While for the nanostructures in acetonitrile with PS staying inside the core, the insulation impact of the PS block would be weakened, and therefore the charge transport become more efficient. That also explains that the film made from the homogeneous solution has a less extent of optical attentuation because the PS blocks randomly disperse in the film. In comparison to the homopolymers without the PS block, the ordered packing of the P(DCH-Ru) in the exterior shell block made from the acetonitrile solution might accelerate the charge transport, and the assembled P(DCH-Ru) displays improved attentuation than the entangled nonassembled P(DCH-Ru) chain in the homopolymer film. Self-assembling block copolymers

dx.doi.org/10.1021/ma200516q |*Macromolecules* 2011, 44, 5146–5154

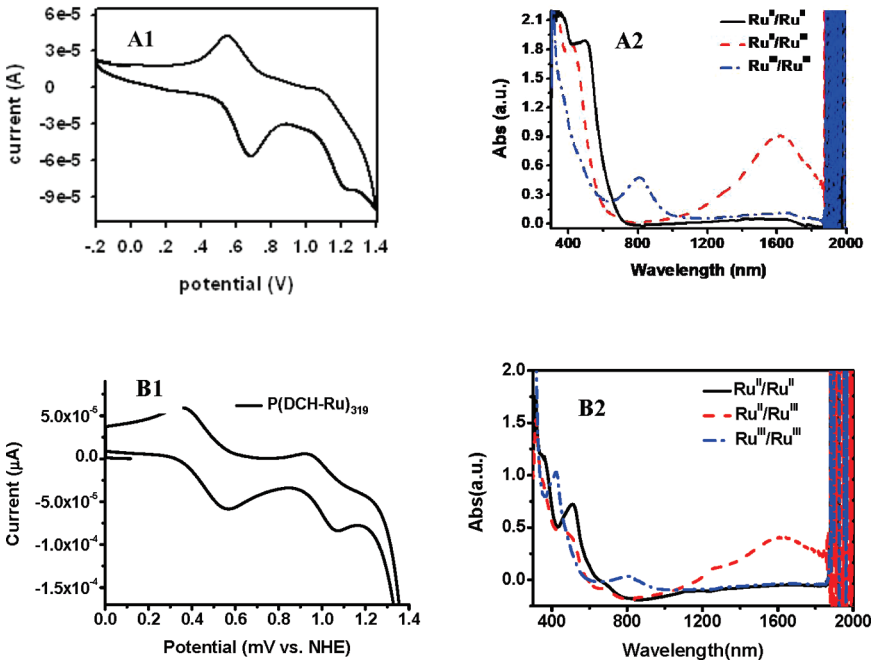

Figure 6. Cyclic voltammogram (A1) at a scan rate of 100 mV/s (with 0.1 M TBAH) and absorption spectra in three oxidation (A2) of thin film cast from complex block copolymer PS_{2076}-*b*-$P(DCH\text{-}Ru)_{417}$ in acetonitrile solution states obtained in DMF using the OTTLE cell (with 0.1 M TBAH). Cyclic voltammogram (B1) and absorption spectra (B2) of the homopolymer were obtained at the same condition as above.

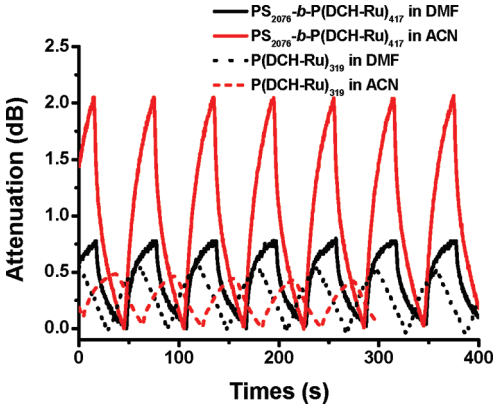

Figure 7. Changes in optical transmission of films cast fromPS_{2076}-*b*-$P(DCH\text{-}Ru)_{417}$ and the homopolymer solution in either acetonitrile or DMF at 1600 nm over time with stepping potentials between −0.3 and +0.8 V.

containing dinuclear Ru polymer blocks thus constitute a promising route to functional supramolecular materials with tailorable optoelectronic properties.

CONCLUSION

In summary, we have reported the synthesis of well-defined diblock copolymers containing dinuclear ruthenium complex via combining two-step sequential nitroxide-mediated radical polymerization and postpolymerization complexation approach. The amphiphilic block copolymers are self-asembling into vesicles in dioxane and spherical micelles in acetonitrile at an initial concentration of 1.0 wt %. Compared with the DCH-Ru complexes and their random copolymers, the packing model of dinuclear Ru chromophores in the core or the shell of the nanostructures have a remarkable effect on the UV−vis absorption properties due to the spatial confinement of the Ru-containing blocks under the local environment. As a result, the block copolymers are solvatochromic in different solvents. The electrochemical and spectroelectrochemical properties of the core−shell micelles of these complex block copolymers in acetonitrile are retained. All the complex block copolymers possess two one-electron oxidation processes and are NIR electrochromic at 1600 nm. The NIR functionalized aggregates could open the door to the long-range order nanomaterials and photonic devices with tunable electroptical properties.

ASSOCIATED CONTENT

Supporting Information. Figures S1−S4. This material is available free of charge via the Internet at http://pubs.acs.org.

AUTHOR INFORMATION

Corresponding Author

*E-mail jz10@pku.edu.cn, Tel 10-86-62754965 (J.Z.); e-mail xhwan@pku.edu.cn, Tel 10-86-62754187 (X.W.).

ACKNOWLEDGMENT

The financial support of the National Natural Science Foundation of China through the Key Program (No. 20834001) and the Research Fund for Doctoral Program of Higher Education of MOE (No. 20060001029) is greatly appreciated.

REFERENCES

(1) De Rosa, C.; Auriemma, F.; Di Girolamo, R.; Pepe, G. P.; Napolitano, T.; Scaldaferri, R. *Adv. Mater.* **2010**, *22*, 5414–5419.

(2) Segalman, R. A.; McCulloch, B.; Kirmayer, S.; Urban, J. J. *Macromolecules* **2009**, *42*, 9205–9216.
(3) Kang, Y. J.; Walish, J. J.; Gorishnyy, T.; Thomas, E. L. *Nature Mater.* **2007**, *6*, 957–960.
(4) Canary, J. W. *Chem. Soc. Rev.* **2009**, *38*, 747–756.
(5) Chen, X. L.; Jenekhe, S. A. *Macromolecules* **1996**, *29*, 6189–6192.
(6) Jenekhe, S. A.; Chen, L. X. *Science* **1998**, *279*, 1903–1907.
(7) Sonmez, G.; Sonmez, H. B.; Shen, C. K. F.; Jost, R. W.; Rubin, Y.; Wudl, F. *Macromolecules* **2005**, *38*, 669–675.
(8) Lim, Y. T.; Kim, S.; Nakayama, A.; Stott, N. E.; Bawendi, M. G.; Frangioni, J. V. *Mol. Imaging* **2003**, *2*, 50–64.
(9) Kim, S.; Lim, Y. T.; Soltesz, E. G.; De Grand, A. M.; Nakayama, A.; Parker, J. A.; Mihaljevic, T.; Laurence, R. G.; Dor, D. M.; Cohn, L. H.; Bawendi, M. G.; Frangioni, J. V. *Nature Biotechnol.* **2004**, *22*, 93–97.
(10) Sonmez, G.; Schwendeman, I.; Schottland, P.; Zong, K.; Reynolds, J. R. *Macromolecules* **2003**, *36*, 639–647.
(11) Miller, L. L.; Zhong, C.-J.; Kasai, P. *J. Am. Chem. Soc.* **1993**, *115*, 5982–5990.
(12) Kim, Y. H.; Jeong, D. H.; Kim, D.; Jeong, S. C.; Cho, H. S.; Kim, S. K.; Aratani, N.; Osuka, A. *J. Am. Chem. Soc.* **2001**, *123*, 76–86.
(13) Groenendaal, L.; Jonas, F.; Freitag, D.; Pielartzik, H.; Reynolds, J. R. *Adv. Mater.* **2000**, *12*, 481–494.
(14) Ng, D. K. P.; Jiang, J. *Chem. Soc. Rev.* **1997**, *26*, 433–442.
(15) Nyokong, T.; Furuya, F.; Kobayashi, N.; Du, D.; Liu, W.; Jiang, J. *Inorg. Chem.* **2000**, *39*, 128–135.
(16) Almlof, J. E.; Feyereisen, M. W.; Jozefiak, T. H.; Miller, L. L. *J. Am. Chem. Soc.* **1990**, *112*, 1206–1214.
(17) Crutchley, R. *Adv. Inorg. Chem.* **1994**, *41*, 273–325.
(18) Kasack, V.; Kaim, W.; Binder, H.; Jordanov, J.; Roth, E. *Inorg. Chem.* **1995**, *34*, 1924–1933.
(19) Kaim, W.; Kasack, V.; Binder, H.; Roth, E.; Jordanov, J. *Angew. Chem., Int. Ed.* **1988**, *27*, 1174–1176.
(20) Wang, Z. Y.; Zhang, J.; Wu, X.; Birau, M.; Yu, G.; Yu, H.; Qi, Y.; Desjardins, P.; Meng, X.; Gao, J. P.; Todd, E.; Song, N.; Bai, Y.; Beaudin, A. M. R.; LeClair, G. *Pure Appl. Chem.* **2004**, *76*, 1435–1443 (Absorbing NIR Material).
(21) Xun, S.; Zhang, J.; Li, X.; Ma, D.; Wang, Z. *Synth. Met.* **2008**, *158*, 484–488.
(22) Xun, S.; LeClair, G.; Zhang, J.; Chen, X.; Gao, J. P.; Wang, Z. Y. *Org. Lett.* **2006**, *8*, 1697–1700.
(23) Qi, Y.; Desjardins, P.; Meng, X. S.; Wang, Z. Y. *Opt. Mater.* **2003**, *21*, 255–263.
(24) Qi, Y.; Desjardins, P.; Wang, Z. Y. *J. Opt. A: Pure Appl. Opt.* **2002**, *4*, S273–S277.
(25) Qi, Y.; Wang, Z. Y. *Macromolecules* **2003**, *36*, 3146–3151.
(26) Qi, Y.; Desjardins, P.; Birau, M.; Wu, X.; Wang, Z. Y. *Chin. J. Polym. Sci.* **2003**, *21*, 147–152.
(27) Wang, S.; Li, X.; Xun, S.; Wang, X.; Wang, Z. Y. *Macromolecules* **2006**, *39*, 7502–7507.
(28) Hawker, C. J.; Barclay, G. G.; Orellana, A.; Dao, J.; Devonport, W. *Macromolecules* **1996**, *29*, 5245–5254.
(29) Sullivan, B.; Salmon, D.; Meyer, T. *Inorg. Chem.* **1978**, *17*, 3334–3341.
(30) Halperin, A.; Tirrel, M.; Lodge, T. P. *Adv. Polym. Sci.* **1992**, *100*, 31–71.
(31) Gao, Z.; Varshney, S. K.; Wong, S.; Eisenberg, A. *Macromolecules* **1994**, *27*, 7923–7927.
(32) (a) Zou, G.; Fang, K.; He, P.; Lu, W. *Thin Solid Films* **2004**, *457*, 365–371. (b) Czikkely, V.; Forsterling, D. H.; Kuhn, H. *Chem. Phys. Lett.* **1970**, *6*, 207–210.
(33) (a) Bergman, S. D.; Goldberg, I.; Barbieri, A.; Barigelletti, F.; Kol, M. *Inorg. Chem.* **2004**, *43*, 2355–2367. (b) Bergman, S. D.; Goldberg, I.; Barbieri, A.; Kol, M. *Inorg. Chem.* **2005**, *44*, 2513–2523. (c) Stadler, A.-M.; Puntoriero, F.; Campagna, S.; Kyritsakas, N.; Welter, R.; Lehn, J.-M. *Chem.—Eur. J.* **2005**, *11*, 3997–4009. (d) Ceroni, P.; Credi, A.; Balzani, V.; Campagna, S.; Hanan, G. S.; Arana, C. R.; Lehn, J.-M. *Eur. J. Inorg. Chem.* **1999**, 1409–1414. (e) Encinas, S.; Flamingni, L.; Barigelletti, F.; Constable, E. C.; Housecroft, C. E.; Schofield, E. R.; Figgemeier, E.; Fenske, D.; Neuburger, M.; Vos, J. G.; Zehnder, M. *Chem.—Eur. J.* **2002**, *1*, 137–150.